Pak. j. sci. ind. res. Ser. A: phys. sci. 2025 **68A**(1) 8-14

First Principles Investigation to Explore Effects of Thulium Doping on Electronic Properties of ZnO

Abdul Majid[a]*, Alia Jabeen[a] and Muhammad Farooq[a]
[a]Department of Physics, University of Gujrat, Gujrat, Pakistan

(received January 6, 2023; revised October 14, 2023; accepted November 14, 2023)

Abstract. The electronic along with the electronic properties of pure zinc oxides (ZnO) and Thulium (Tm) doped ZnO were studied by utilizing the density functional theory. The periodically arranged bulk crystalline structures were investigated for single point precision within framework of Perdew-Burke-Ernzerhof functional in generalized gradient approximation (GGA-PBE) implemented in amsterdam density functional BAND (ADF-BAND). The computed band gap of the pristine ZnO is ~1.36 eV and after doping the band gap increased to 1.6 eV and new energy levels 4*f* orbitals are produced in the band gap of ZnO. The pristine ZnO offers zero spin polarization whereas the Tm doped ZnO shows considerable spin polarization in the 4*f* orbitals of the thulium atom which shows the ferromagnetic behaviour of the material. The modifications in electronic, magnetic as well as optical properties of ZnO induced after Tm doping are studied in detail. The band structure showing impurity levels is modeled.

Keywords: density function theory, amsterdam density functional, zinc oxide, Tm doped ZnO, ferromagnetic, electronic properties

Introduction

Zinc oxide (ZnO) is considered to be a versatile semiconductor because of having properties for use in blue/UV optoelectronics, spintronic and sensor applications (Kowalik *et al*., 2007). It is usually found in polycrystalline form and is extensively used in different areas of life including *e.g*. ointment, pigment, facial powder, lubricant additives, sunscreen, catalyst, paint, piezoelectric transducer, varistors as well as transparent conducting material. Frontier characteristics of ZnO involve luminescent, photoconductive, photochemical, semiconducting, and ferrite (Özgür *et al*., 2010).

ZnO is one of the promising semiconductor solids that shows versatile applications within the piezoelectric devices, spin-electronics, transparent electronics, chemical sensors and ultraviolet (UV) light emitters (Athar, 2015). As ZnO can be found in the form of large single crystals so, this is a huge advantage over the gallium nitride (GaN). For instance, the GaN are grown on the sapphire having a mismatch of 16%, which results the huge concentration of defects almost 10^6-10^9 cm^{-2} (Ryu, 2007). Whereas the ZnO is normally grown on the native substrate and concentration of defects is reduced, so the performance of ZnO in the electronics devices is much better than the GaN (Perdew and Kurth, 1998). In the fabrication and forming the design of the device the ZnO has another advantage over the GaN.

The crystals of ZnO are intrinsically n-type, yet the doping of p-type material in the ZnO is still a question for the researcher and also the features for producing a stable p-type doping are yet to be known (Ng *et al*., 2018; Brauer *et al*., 2011). The control of conductivity in the ZnO is still the problem of concern even the minor amount of native impurities and point defects can bring a lot of changes in the electrical and optical properties. That is why, the understanding of the part of native impurities as well as defects are the major factors within controlling the conductivity of ZnO (Sato and Katayama- Yoshida, 2001). For decades it had been considered that the unintentional n-type conductivity within ZnO strongly depend upon vacancies of oxygen and zinc interstitials. However, by using the density functional theory along with the optical detection of electron paramagnetic resonance measurements over the fine quality ZnO crystal reveals that intrinsic defects do not responsible for this kind of behavior of ZnO (Yun *et al*., 2004). Role of some other point defects has also been investigated in this regard (Huang and Guo *et al*., 2020; Fukumura *et al*., 2001). It has been revealed that O in ZnO is replaced by the H (Lany and Zunger, 2007; Lany and Zunger, 2005) and this substitution of H is more stable as compared to the interstitial H along

*Author for correspondence;
E-mail: abdulmajid40@yahoo.com

with the fact that they also have the explanation of the stability of n-type conductivity as well as change of stability in the presence of the partial pressure of oxygen.

By considering the II-VI semi-conductors, ZnO is one of the exciting material these days. The ZnO has gained great concentration in some current years as it offers the better theoretical understanding along with the superior process. As a result, it shows potential towards the novel applications such as spintronic, nanotechnology and opto-electronics (Panda and Tseng, 2013). By comparing with other metal oxides semiconductors, the said materials offer higher redox potential, excellent chemical as well as physical stability along with being harmless (Singh *et al*., 2019). Because of being semiconductor, the ZnO offers the photocatalytic activity and gas sensing applications, which is based on the several factors like synthesis method, purity of phase, size of crystalline, dopants nature and surface area (Huang *et al*., 2014; Olaru *et al*., 2014). Furthermore, the sensing capability is based on the difference experienced in the carrier defects in the presence and absence of sensing gases. Such carrier defects are chiefly those of Oxygen vacancies, which could be remarkably enhanced through doping and in-turn increases the performance of the respective devices. The optoelectronic device's performance, that is based on the hole or electron mobility in distinctive type of semiconductor could be enhanced through the increment in the mobility.

There has been a lot of research on study of doping into ZnO and this material is regarded as a good host for the doping of distinct elements. Several groups have doped ZnO with 3d, 4d, 5d to 4f transition metals to modify its properties (Sato and Katayama-Yoshida, 2001). In general, the insertion/doping of TM would modify the band gap and tune this for suitable level, acceptor as well as donor defects conductivity, mobility and various properties associated with the magnetic and optical characteristics (Singh *et al*., 2019). The investigation on yellow luminescence of ZnO single crystal and also study the effects of doping with different Li isotopes has also been performed (Corolewski *et al*., 2016). The investigation of the impact of distinct co-activators over ZnO luminescence like Li, N, Na and P at distinct implantation energies was studied (Pierce and Hengehold, 1976). The doping of Bi as well as Mn in ZnO was studied by Gracia *et al*. (1987) they also blue green photoluminescence of the said material.

The ZnO doped with the rare earth had been reported to have several prospects for device grade applications (Zhang *et al*., 2011). The photoluminescence properties of the rare earth element (Eu) doped ZnO has been studied and indicted the fact that dopant concentration dependent rise of luminescence intensity (Yoon *et al*., 2012). Though a lot of work was done on the doping of rare earth metals to study optical and optoelectronic properties but minute efforts have been reported on thulium doped ZnO (Tm-ZnO). This work is motivated to carry out the detailed investigations of the magnetic characteristics in the light of electronic characteristics of Tm-ZnO in bulk periodicity by utilizing the density functional theory based calculations.

Materials and Methods. The computation performed were executed by utilizing density functional theory (DFT) which is based on scheme by Kohn-Sham (KS), according to which for every interacting electron having exterior potential, the local potential is available in a way that density of the non-interacting system is equal to density of relevant interacting system (Sholl and Steckel, 2023). For this purpose, the amsterdam density functional (ADF-BAND) code that is widely utilized for periodic systems. In order to apply these considerations, we used widely used approximation of local density approximation (LDA). The LDA approximates true in homogeneous system that may be described by homogeneous electron gas. The described method is simple approximation and is expected to work for systems having slowly varying density. There are also some notable failures of the said level of theory that incorporates the famous under estimation of the band gaps for semiconductors as well as insulators because of the unavailability of the derivative discontinuities within the said functional *i.e*. LDA. The generalized gradient approximation (GGA) is alternate and it proposes functional which improve their conduct at large gradients such that to conserve the preferential characteristics (Perdew *et al*., 1996). Numerous forms for such function have been used out of which three of the most widely used ones that were proposed by Perdew (1986) and also again in 1996.

The wurtzite (WZ) configuration has symmetry number=186 and space group ($P6_3mc$). We selected experimental lattice constants a=3.24992Å; c=5.20658Å and u=0.375Å as starting parameters. By using the above parameter, we construct the WZ structure of ZnO which is shown in the Fig 1. (a,b and c)

We generated 2×2×1 super cell of WZ structure of ZnO to carry out different calculations. All computations

were performed in the framework of DFT executed within BAND program of amsterdam density functional (ADF) package. To perform the computations, a 3 k-space points mesh within the irreducible brillouin zone (IBZ) were utilized to achieve the self consistency during cycles consisting of 50 iterations for WZ structure. We used DZ basis sets and k-space integration was carried out with 18 k-points for density of states (DOS) and band diagram computations. An accuracy parameter of 3.5 was used with self consistent error of 0.61 $x10^{-8}$ eV. In this work we used the GGA-PBE (Perdew-Burker-Ernzerhof) functional and single point precision of DFT to calculate the DOS and energy band gap of pure (pristine) as well as Tm doped ZnO. Figure 1. (a,b and c) shows top and side views of bulk ZnO.

Furthermore, the energy convergence criteria were taken as $1x10^{-6}$ eV for all the calculations.

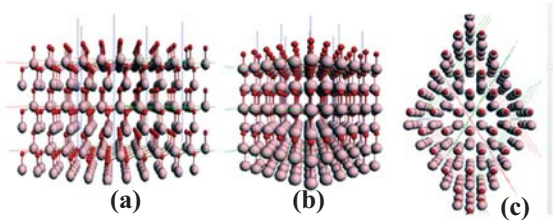

Fig. 1. (**a,b** and **c**). The optimized structure of bulk ZnO along X-axis, Y-axis and Z-axis respectively.

Results and Discussions

Pure ZnO. The Fig. 2(a) exhibits the band structure of pristine WZ ZnO that presents the direct band gap of ~1.3 eV. This value is strongly underestimated, when compared with band gap as attained by experimental setup that is ~3.4 eV because of the famous inaccuracy of the DFT calculations. The top of valance band is made of major contribution from O 2p whereas minima of conduction band (CBM) is made of 4s orbitals from Zn atom. The valance band (VB) consists of three non-degenerate energy levels splitted due the crystal field effects. Figure 2 (b) shows energy splitting between the A and B orbitals of the valance band due the spin orbit coupling effect.

The calculated density of states indicated mixing of the s and p orbitals of Zn and O that causes the transformation of the charge and shifts the center of gravity towards the low energy region *i.e*. towards the oxygen atom. No spin polarization was observed.

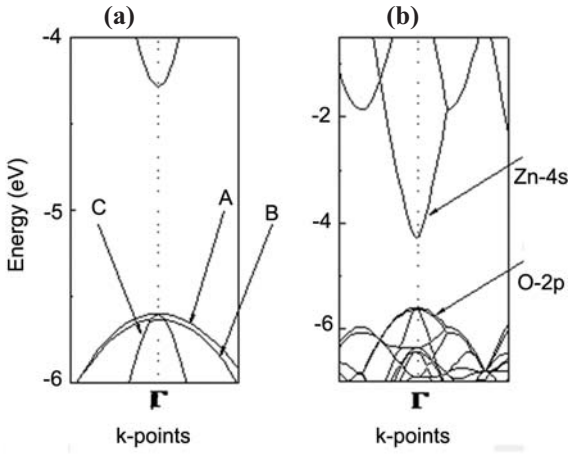

Fig. 2. The band diagram of (**a**) Pristine ZnO (**b**) The splitting of energy levels of the VB of pristine ZnO.

Tm doped ZnO. The DOS chart of Tm doped ZnO is presented in Fig. 3. The lower part of the VB in energy range of -9.4 eV to -5.4 eV, comprised of 3d orbitals from Zn atom. The results showed the absence of any anti symmetric spin that's why they do not contribute towards magnetic characteristics of the said material. The maxima of valence band (VBM) found at -2.787 eV is comprised of 2p orbitals of oxygen. These findings are in great accordance with the reported literature (Yun *et al*., 2004).

Besides these, like that of pristine ZnO, the CBM is composed of 4s orbitals of Zn just below 5d orbitals of

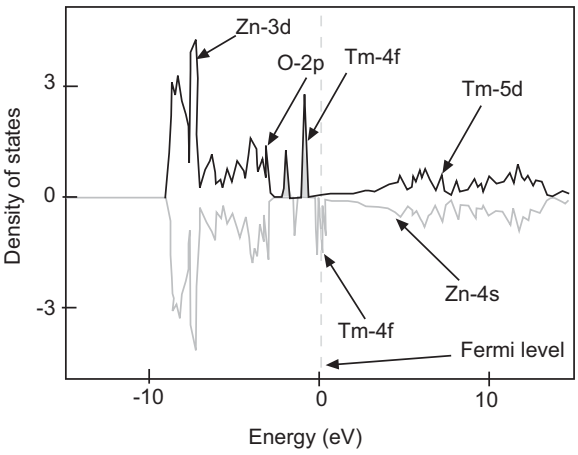

Fig. 3. The density of state (DOS) of Tm doped ZnO, where black and red coloured curves shows the spin up and spin down.

Tm. The tail of the conduction band comprises 6s orbital of thulium. From the figure it is also clear that Fermi level has been shifted towards the conduction band and spin polarized 4f states appeared inside band gap.

Figure 4. shows partial density of states (pDOS) of Tm doped ZnO (Tm-ZnO). In this case, 4f gap states will have an influence on the electronic characteristics of the material. Due to highly localized character of 4f states, the probability of coupling with the s, p and d states of the host material is minimum. However, a small hybridization of 4f states with Zn s states is observed.

Figure 5. represents band diagram of the Tm-ZnO. It is seen that like pristine ZnO the Tm doped ZnO exhibits also as a direct band gap material yet the band gap value is improved to 1.6 eV in comparison with the ~1.36 eV of pure ZnO. The increase in band gap is assigned to Burstein Moss effect.

The band gap has been increased because the iconicity of the material has been increased. The values of electronegativity of O, Zn as well as Tm atoms are 3.44, 1.65 and 1.25 respectively. The electronegativity difference within the Zn-O bond is 1.75 while the Tm-O bond offers the difference in electronegativity of

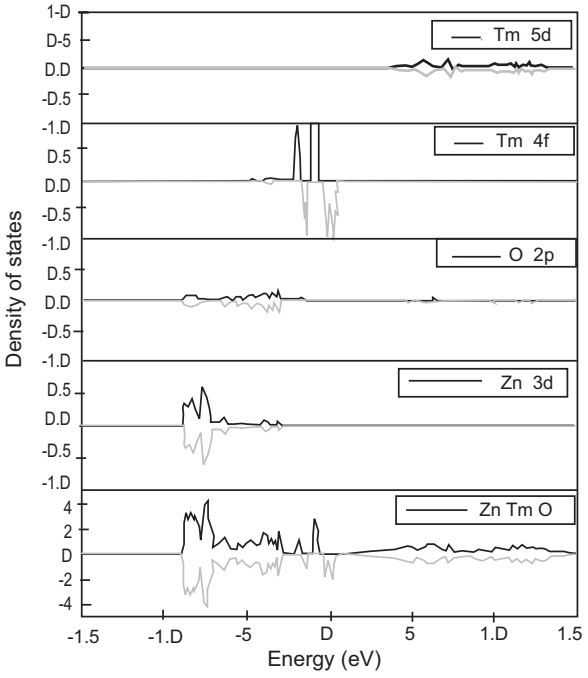

Fig. 4. The partial and total density of states of Tm doped-ZnO.

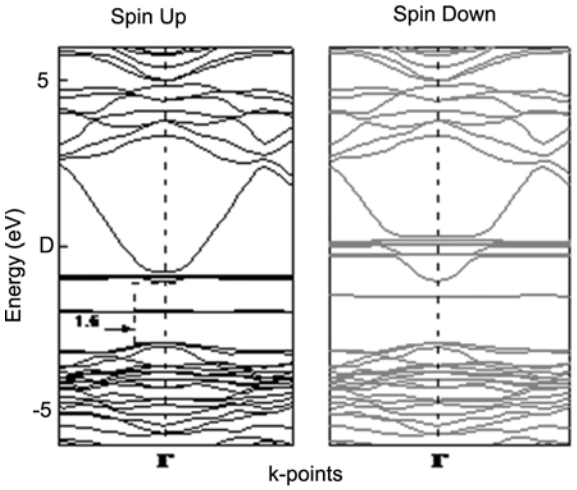

Fig. 5. The band structure Tm doped ZnO showing the Spin-up and Spin-down configurations.

~2.19. By the well-known fact, the bond contains the more than 50% ionic character if the electronegativity difference is more than 1.7. So Tm-O bond is more ionic as compared to the Zn-O bond (Sujatha *et al*., 2019). Also the ionic bond is stronger than the covalent bond so the Tm-ZnO exhibits stronger bond in comparison to the pristine ZnO. Furthermore, formation energy as computed for pristine WZ-ZnO as well as the Tm-ZnO is -71.155 eV and -79.995 eV respectively. Another observation is shift of Fermi level, that moved towards the CB in case of doping which points to n-type conductivity in it (Katayama-Yoshida and Sato, 2003).

The composition of the valence band is 2p and 3d orbitals of the oxygen and Zn atoms respectively. The top part is made up of 2p orbitals of oxygen and preceding part is 3d orbitals of Zn. The CB is built by the 4s orbitals by Zn. However, the 4f states of Tm atom are produced in the band gap region. They are below the Fermi level in the spin-up as well as the spin-down except two states of 4f which is above the Fermi level in spin down band gap, which shows that these are unoccupied states while all the other states which are below the Fermi level, are occupied.

When the Tm is doped within the crystalline ZnO the splitting of f orbitals occurs because of the crystal field splitting and spin orbital coupling effects. The f orbitals within the tetrahedral domain split into 3 orbitals from which one is singly non-degenerate a1 while the

remaining 2 are triply degenerate *i.e*. t_1 as well as t_2 states (El Hachimi *et al*., 2014). This splitting is shown in the Fig. 6 in terms of the DOS as well as energy. In the Fig. 7, DOS of spin-up as well as spin-down each 4f orbital separately, DOS of total 4f orbital and the DOS of the Tm-ZnO are shown. This splitting can be viewed in another way using the band gap diagram. Here the comparison of DOS in terms of spin up, spin down band gap of the Tm doped WZ ZnO has been drawn.

In Fig. 7. the DOS of each 4f orbital separately, total DOS of 4f orbital and DOS of Tm doped ZnO has been shown. In the partial density of states of 4f the black peaks describe the filled orbitals and red peaks show unfilled states. Using the calculated results, the predicted energy level diagram of Tm-ZnO showing 4f levels is plotted in Fig. 8.

As there are fourteen electrons in the 4f orbitals and in each subshell of 4f there are two electrons according to the Pauli's Exclusion Principle. But here in this diagram we have represented splitting of each subshell when the atom is placed in the crystalline material.

Conduction band is put at 0 eV, whereas the red portion shows the impurity level above which is the conduction band (CB). Fermi level is at 3.00 eV. Lowest occupied electrons after the conduction band are at 1.057 with respect to the valence band. Actually these two electrons are linked two different subshells of f orbitals *i.e*. $3x^2y$-y^3 and x^3-$3xy^2$ having the spin up motion. The spin down electrons of these subshells are at 1.46 and 3.10 eV respectively. Thus the violation of the Pauli's Exclusion principle is avoid. Similarly next three electrons with spin up motion are from $z(x^2$-$y^2)$, z^3 and

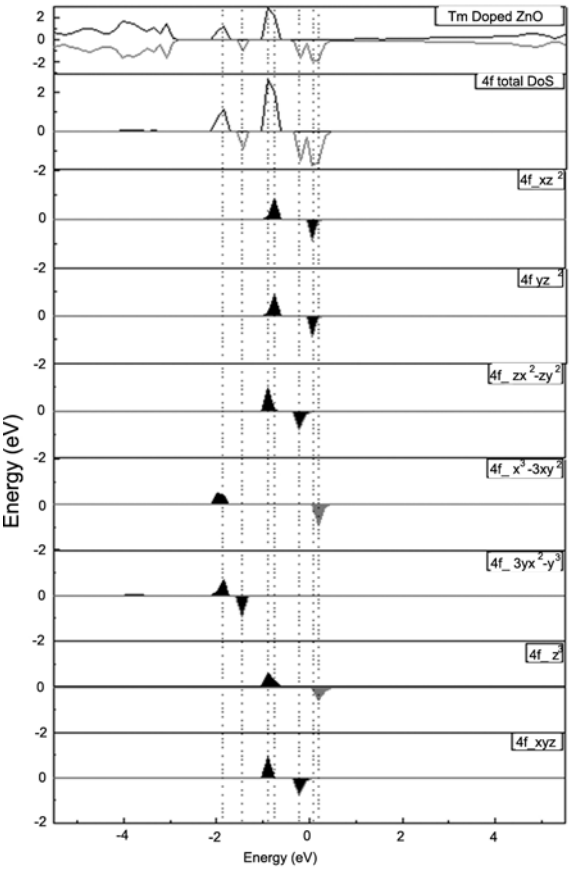

Fig. 7. Splitting of 4f orbital of Tm after doping in the WZ ZnO.

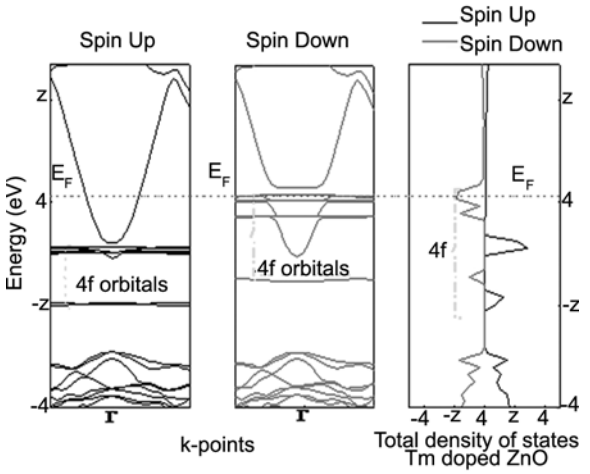

Fig. 6. Appearance of impurity induced gap states in ZnO.

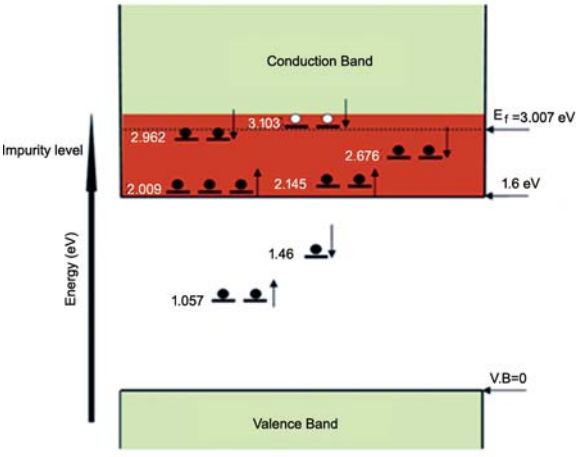

Fig. 8. Energy level diagram of 4f orbitals of Tm in WZ ZnO.

xyz, are at 2.01 eV following by two electrons of xz^2 and yz^2 having spin up motion at 2.14 eV. Spin down electrons of $z(x^2-y^2)$ and xyz are at 2.67 eV, while at 2.96 eV, electrons are from the xz^2 and yz^2 states having spin up. These electrons are just lower than the Fermi level. Two states are above the Fermi level shown the energy 3.10 eV with spin down direction. These states will be empty because these are above the fermi level. The twelve sub-shells are totally filled, however the two sub-shells by 4f orbitals are totally vacant. Such vacant states are above the Fermi level of about ~3.10 eV. Also, such states would be filled through the electrons present in the spin down state. Such vacant states are z3 as well as x^3-3xy^2 which further verifies that the nature of doping, which is n-type in current situation.

Conclusion

The electronic properties along with the optical characteristics of the pristine as well as Tm-WZ ZnO were investigated in detail utilizing the DFT. It was observed that after doping the band gap is increased a little bit and spin polarization of 4f orbitals takes place leading to the splitting. This polarization makes the magnetic material and makes it possible to use it in the spintronic devices and diluted magnetic semiconductors which are the latest devices in the electronics field.

Conflict of Interest. The authors declare that they have no conflict of interest.

It is stated that there are no competing or conflict of interests to declare by the authors of this manuscript.

References

Athar, T. 2015. *Smart Precursors for Smart Nanoparticles Emerging Nanotechnologies for Manufacturing*, 444-538 pp. Elsevier., Amsterdam, Netherlands.

Brauer, G., Kuriplach, J., Ling, C., Djurišic, A. 2011. Activities towards p-type doping of ZnO. In: *Proceedings International Workshop on Positron Studies of Defects (PSD 08)*, pp. 0120-02. IOP Publishing, Bristol, United Kingdom.

Corolewski, C.D., Parmar, N.S., Lynn, K.G., McCluskey, M.D. 2016. Hydrogen-related complexes in Li-diffused ZnO single crystals. *Journal of Applied Physics*, **120:** 035703.

El Hachimi, A., Zaari, H., Benyoussef, A., El Yadari, M., El Kenz, A. 2014. First principles prediction of the magnetism of 4f rare-earth-metal-doped wurtzite zinc oxide. *Journal of Rare Earths*, **32:** 715-721.

Fukumura, T., Jin, Z., Kawasaki, M., Shono, T., Hasegawa, T., Koshihara, S., Koinuma, H. 2001. Magnetic properties of Mn-doped ZnO. *Applied Physics Letters*, **78:** 958-960.

Garcia, J., Remon, A., Piqueras, J. 1987. Influence of Bi and Mn on the green luminescence of ZnO ceramics. *Journal of Applied Physics*, **62:** 3058-3059.

Huang, M., Weng, S., Wang, B., Hu, J., Fu, X., Liu, P. 2014. Various facet tunable ZnO crystals by a scalable solvothermal synthesis and their facet-dependent photocatalytic activities. *The Journal of Physical Chemistry C*, **118:** 25434-25440.

Huang, Y., Guo, M., Li, J. 2020. Multiscale defect responses in understanding degradation in zinc oxide varistor ceramics. *Ceramics International*, **46:** 22134-22139.

Katayama-Yoshida, H., Sato, K. 2003. Materials design for semiconductor spintronics by ab initio electronic-structure calculation. *Physica B: Condensed Matter*, **327:** 337-343.

Kowalik, I.A., Guziewicz, E., Kopalko, K., Yatsunenko, S., Godlewski, M., Wójcik, A., Osinniy, V., Krajewski, T., Story, T., Lusakowska, E. Paszkowicz, W. 2007. Extra-low temperature growth of ZnO by atomic layer deposition with diethylzinc precursor. *Acta Physica Polonica A*, **112:** 401-406.

Lany, S., Zunger, A. 2005. Anion vacancies as a source of persistent photoconductivity in II-VI and chalcopyrite semiconductors. *Physical Review B*, **72:** 035215.

Lany, S., Zunger, A. 2007. Dopability, intrinsic conductivity, and non-stoichiometry of transparent conducting oxides. *Physical Review Letters*, **98:** 045501.

Ng, Z.-N., Chan, K.-Y., Muslimin, S., Knipp, D. 2018. P-type characteristic of nitrogen-doped ZnO films. *Journal of Electronic Materials*, **47:** 5607-5613.

Olaru, N., Calin, G., Olaru, L. 2014. Zinc oxide nanocrystals grown on cellulose acetate butyrate nanofiber mats and their potential photocatalytic activity for dye degradation. *Industrial & Engineering Chemistry Research*, **53:** 17968-17975.

Özgür, Ü., Hofstetter, D., Morkoc, H. 2010. ZnO devices and applications: a review of current status and future prospects. *Proceedings of the IEEE*, **98:** 1255-1268.

Panda, D., Tseng, T.Y., 2013. One-dimensional ZnO nanostructures: fabrication, optoelectronic properties and device applications. *Journal of Materials Science*, **48:** 6849-6877.

Perdew, J.P., Burke, K., Ernzerhof, M. 1996. Generalized gradient approximation made simple. *Physical Review Letters*, **77:** 3865.

Perdew, J.P., Kurth, S. 1998. Density functionals for non-relativistic coulomb systems. Density Functionals: Theory and Applications: In: *Proceedings of the Tenth Chris Engelbrecht Summer School in Theoretical Physics*, pp.88-59, Cape Town south Africa.

Pierce, B.J., Hengehold, R.L. 1976. Depth resolved cathod-oluminescence of ion implanted layers in zinc oxide. *Journal of Applied Physics*, **47:** 644-651.

Ryu, Y.T., Lee, J.A., Lugbuban, H.W., White, B.J., Kim, Y.S., Park, C.J.Y. 2007. Excitonic ultraviolet lasing in ZnO-based light emitting devices. *Applied Physics Letter*, **88:** 241108.

Sato, K., Katayama-Yoshida, H. 2001. Electronic structure and ferromagnetism of transition-metal-impurity-doped zinc oxide. *Physica B: Condensed Matter*, **308:** 904-907.

Sato, K.S.K., Katayama-Yoshida, H.K.-Y. H. 2001. Stabilization of ferromagnetic states by electron doping in Fe-, Co-or Ni-doped ZnO. *Japanese Journal of Applied Physics*, **40:** L334.

Sholl, D. S., Steckel, J. A. 2023. *Density Functional Theory: A Practical Introduction*, 238pp. John Wiley & Sons., USA.

Singh, P., Kumar, R., Singh, R.K. 2019. Progress on transition metal-doped ZnO nanoparticles and its application. *Industrial and Engineering Chemistry Research*, **58:** 17130-17163.

Sujatha, K., Israel, S., Anzline, C., Ali, K.S., Sheeba, R., Rajkumar, P.R. 2019. Analysis of oxygen bonding with metals of different oxidation states from experimental charge density distribution. *Physica B: Condensed Matter*, **555:** 21-31.

Yoon, H., Hua Wu, J., Hyun, M.J., Sung, L.J., Ju, J.-S., Keun, K.Y. 2012. Magnetic and optical properties of monosized Eu-doped ZnO nanocrystals from nanoemulsion. *Journal of Applied Physics*, **111:** 07B523.

Yun, S.Y., Cha, G.B., Kwon, Y., Cho, S., Hong, S.C. 2004. First-principles calculations on magnetism of transition metal doped zinc oxide. *Journal of Magnetism and Magnetic Materials*, **272:** E1563-E1564.

Zhang, X.-H., Chen, J., Wu, Y., Xie, Z., Kang, J., Zheng, L. 2011. A simple route to fabricate high sensibility gas sensors based on erbium doped ZnO nanocrystals. *Colloids and Surfaces A: Physicochemical and Engineering Aspects*, **384:** 580-584.